Galaxy Masses as Constraints of Formation Models
Proceedings IAU Symposium No. 311, 2014
M. Cappellari & S. Courteau, eds.

doi:10.1017/S1743921315003385

ATLAS^{3D} Stellar Population Gradients

Harald Kuntschner

European Southern Observatory, Karl-Schwarzschild-Strasse 2, 85748 Garching, Germany.
email: hkuntsch@eso.org

Abstract. We present stellar population gradients of early-type galaxies from the ATLAS^{3D} survey: a complete, volume-limited multi-wavelength survey of 260 early-type galaxies in the local 42 Mpc volume. Using emission-corrected spectra integrated within elliptical annuli we measure line-strength indices and apply single stellar population (SSP) models to derive SSP-equivalent values of stellar age, metallicity, and alpha enhancement as function of radius. For all galaxies we derive basic linear stellar population gradients versus radius $\log(R/R_e)$. These gradients are examined on their own and versus three mass-sensitive parameters: K-band luminosity M_K, velocity dispersion within one effective radius $\log \sigma_e$, and our dynamical mass M_{JAM}. We find a correlation between positive age gradients (younger centre) and steeper negative metallicity gradients with a Spearman rank correlation coefficient of -0.46 and a significance of 7.65×10^{-15}. Furthermore, we find a robustly estimated mean metallicity gradient of $\Delta[Z/H] = -0.37 \pm 0.01$ for the sample with a significant trend for more massive galaxies to have shallower profiles. While there is no *clear* distinction between fast and slow rotators or signs of environmental influence, we do detect a significantly larger range of [Z/H]-gradients towards low mass galaxies.

Keywords. galaxies: elliptical and lenticular, cD - galaxies: evolution - galaxies: formation

1. Introduction

The spatial distribution of stellar population properties (e.g. age, metallicity and more detailed chemical composition information) in galaxies holds important clues to the formation and evolution mechanisms which shaped these galaxies. Competing formation scenarios and the physical processes involved predict significantly different radial distributions. Thereby, offering the opportunity to use observed stellar population gradients in galaxies as a discriminating tool for the various formation and evolution scenarios.

The aim of this contribution is to provide new insights into stellar population gradients by making use of the high S/N IFU observations of a complete, magnitude limited sample of 260 nearby ETGs in the ATLAS^{3D} survey (Cappellari *et al.* 2011). From the final SAURON datacubes, which were adaptively binned to a minimum signal-to-noise ratio threshold of 40, a number of quantities were derived. Gas and stellar kinematics were extracted via a pixel fitting algorithm. Emission-corrected absorption line indices in the Lick/IDS system (Trager *et al.* 1998) were derived for each bin following the procedures described in Kuntschner *et al.* (2006). Due to our limited wavelength range (4800 – 5380 Å) only the Hβ, Fe5015 and Mg b indices can be measured over the full spatial extent of the datacubes (see also McDermid *et al.* 2014).

As described in Scott *et al.* (2013), using the ATLAS^{3D} line-strength maps, we constructed radial profiles extracted from elliptical annuli for each galaxy, except for seven objects where the limited spatial extent and/or limited S/N did not warrant derivation of gradients. This leaves a total sample of 253 galaxies for this study. The ellipticity chosen was a global ellipticity measured using the weighted second moments of the surface brightness as described in Krajnović *et al.* (2011). The error on each point for the line-strengths is the rms sum of the measurement errors and the rms scatter within each

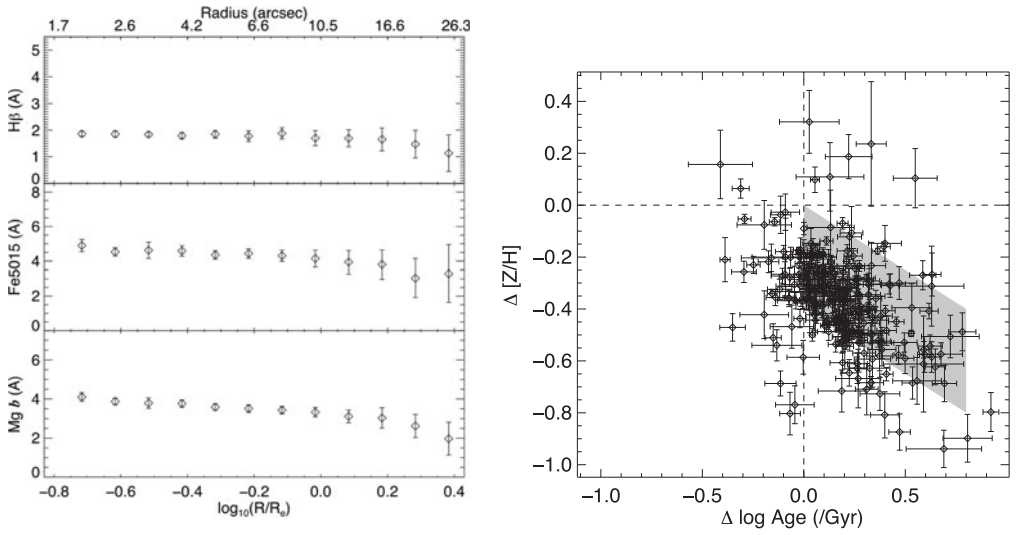

Figure 1. Left: Example of line-strength extractions in elliptical annuli as function of radius normalised to the effective radius R_e. The data shown is for NGC 2481. **Right:** Age gradients $\Delta \log \mathrm{Age}$ versus metallicity gradients Δ [Z/H]. The grey shaded area shows the approximate region occupied by the simulations of Hopkins *et al.* (2009, their fig. 29).

annulus. Foreground stars and bad bins due to low S/N were masked in the line-strength maps before extracting the profiles. In Fig. 1 (left) we show an example of the extracted line-strength measurements as function of radius. Averaging along elliptical annuli provides high quality information on the *average* line-strengths gradients but naturally, line-strength information on more detailed spatial scales (e.g. young star forming disks or bars) is largely lost.

2. Results

On average, the galaxies in our sample show negative metallicity gradients with a robustly estimated mean gradient of $\Delta[\mathrm{Z/H}] = -0.37 \pm 0.01(0.22)$ (a robust estimate of the 1-sigma scatter is given in brackets). The average age and [α/Fe] gradients are positive with values of $\Delta \log \mathrm{Age} = 0.18 \pm 0.01(0.19)$ and $\Delta[\alpha/\mathrm{Fe}] = 0.05 \pm 0.01(0.13)$, respectively. While average negative metallicity gradients are found in essentially all studies of ETGs, results for age and [α/Fe] gradients do vary (e.g. Spolaor *et al.* 2010; Rawle *et al.* 2010; Koleva *et al.* 2011). In a first step to better understand the relation of stellar population gradients with other global parameters of the galaxies we explore the relation between gradients and central age and metallicity, here defined as values derived from the central $R_e/8$ aperture (McDermid *et al.* 2014). In previous studies, significant correlations were found for the metallicity gradients as well as the age gradients with central metallicity (e.g. Rawle *et al.* 2010). Furthermore, there is an anti-correlation of the age gradient with central age where younger galaxies show more positive gradients (i.e. younger centres; Kuntschner *et al.* 2010; Koleva *et al.* 2011).

We find a highly significant anti-correlation between the age gradients with the central age (Spearman rank correlation $= -0.49$ with a significance of 9.33×10^{-17}). The on-average positive age gradients can be understood straightforwardly in the hierarchical galaxy formation picture where (multiple) merging and accretion events cause the formation of young stars preferentially in the centre of galaxies (e.g. Hopkins *et al.* 2009).

https://doi.org/10.1017/S1743921315003385 Published online by Cambridge University Press

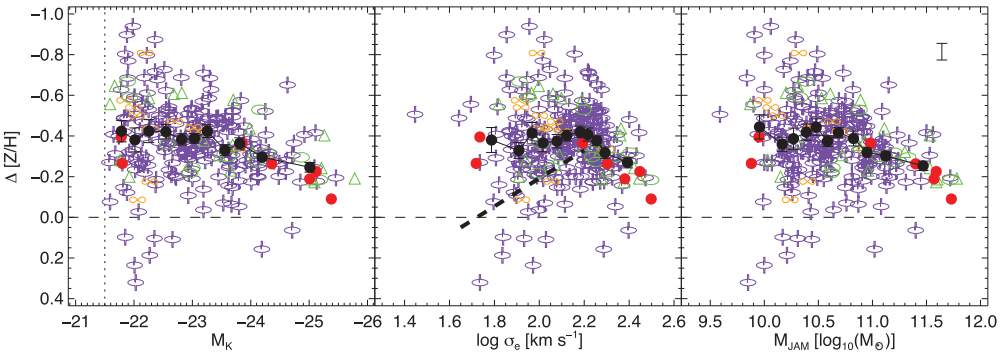

Figure 2. Metallicity gradients Δ [Z/H] are shown for 253 galaxies as function of K-band luminosity M_K, velocity dispersion within one effective radius $\log \sigma_e$, and the dynamical mass M_{JAM}. The global sample selection limited by $M_K = -21.5$ is indicated with a dotted line. Median error bars for gradients are shown in the upper right corner of the M_{JAM} panel. Red circles show galaxies with little or no rotation, green ellipses have complex velocity maps with no specific features, green triangles are KDCs, orange lemniscates have off-centre dispersion peaks indicative of superposed counter-rotating disks. Magenta spindles are the the regular rotators. The black solid symbols show robust estimates of mean values for non-overlapping bins each containing the same number of data points. Errors on those points represent robustly estimated errors on the mean. In each panel we indicate the level of zero (=no) gradient with a dashed line. The thick dashed line in the middle panel represents the tight relation of metallicity gradient with $\log \sigma_e$ found by Spolaor *et al.* (2010).

The correlation is most obvious for the "youngest" systems (with the most recent star-formation) but is still present if only galaxies with luminosity-weighted ages greater than e.g. 6 Gyr are considered (-0.37 with significance of 1.58×10^{-6}). A plausible explanation for the metallicity gradient versus central metallicity correlation also arises from the same scenario where enriched gas leads to the formation of (younger) metal rich *central* regions which steepens the overall gradients (Hopkins *et al.* 2009). If this scenario is correct, then one would expect a correlation between positive age gradients and steeper (more negative) metallicity gradients. Indeed, this is what was found previously (Rawle *et al.* 2010; Koleva *et al.* 2011) and is also true for our sample as shown in Fig. 1 (right). The Spearman rank correlation coefficient is -0.46 with a significance of 7.6×10^{-15}.

In Fig. 2 we present the relation of metallicity gradients versus three indicators of total system mass for our magnitude limited ATLAS^{3D} sample. As proxies for mass we use the integrated K-band magnitude, the velocity dispersion measured within one effective radius R_e and our own dynamical mass (M_{JAM}) estimates (Cappellari *et al.* 2013). There is a general trend of shallower metallicity gradients with increasing mass. Significant scatter is found at all masses perhaps reflecting different merger configurations and merger gas fractions, but there is an increased scatter towards the low mass end. In the $\log \sigma_e$ diagram we see a weak downturn of the relation for $\log \sigma_e < 2.2$, however, this is not as strong as what Spolaor *et al.* (2010, see thick dashed line) found. There is no obvious relation with fast or slow rotators apart from the general mass trend, where the most massive systems have the shallowest gradients and are more likely of slow rotator class.

For galaxies with extreme post-starburst-like signatures, the assumption of a *linear* stellar population gradients with $\log(R/R_e)$ can break down. Furthermore, the luminosity weighted nature and simple SSP approach of our analysis can lead to unphysical interpretations of the observed line-strength distribution for these galaxies. We therefore restrict our analysis now to galaxies with central ages of greater than 4 Gyr leaving 190

https://doi.org/10.1017/S1743921315003385 Published online by Cambridge University Press

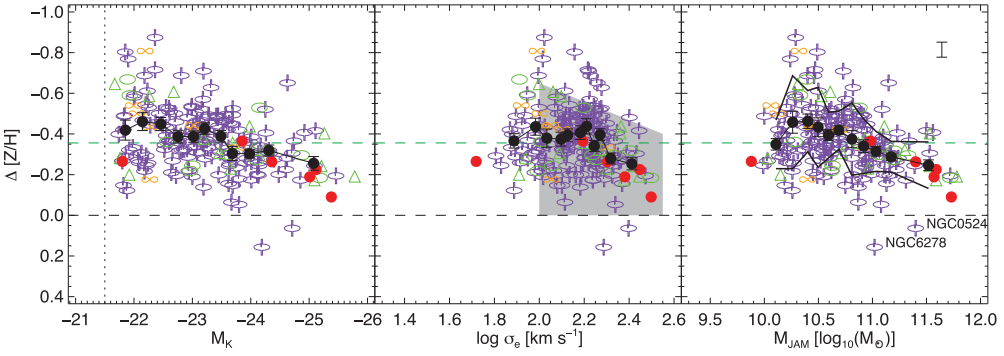

Figure 3. Metallicity gradients Δ [Z/H] are shown as function of K-band luminosity M_K, velocity dispersion within one effective radius $\log \sigma_e$, and dynamical mass M_{JAM}. The sample is restricted to 190 galaxies with central 1/8 Re ages greater than 4 Gyr. The median gradient of -0.36 dex is indicated by the dashed green line. The grey shaded area in the middle panel shows the approximate region occupied by the simulations of Hopkins *et al.* (2009, their fig. 29).

galaxies as shown in Fig. 3. The main relations persist and tighten up (i.e, less scatter), particularly the metallicity gradients versus dynamical mass relation is becoming significantly clearer (Spearman correlation of -0.33; significance 2.16×10^{-6}).

3. Conclusions

We find a significant correlation between positive age gradients (younger centres) and steeper negative metallicity gradients providing evidence in support of gas rich accretion/merging, i.e. that mergers drive gas to the centre, encouraging star formation from the enriched gas. Furthermore, we find a robustly estimated mean metallicity gradient of Δ[Z/H] $= -0.36 \pm 0.01$ for the complete sample with a significant trend for more massive galaxies to have shallower profiles. While there is no *clear* distinction between fast and slow rotators or signs of environmental influence, we do detect a significantly larger range of [Z/H]-gradients towards low mass galaxies; this indicates that gas-rich mergers are more prevalent at lower masses.

Acknowledgements

I acknowledge generous support by the ATLAS^{3D} team.

References

Cappellari, M., Emsellem, E., Krajnović, D., *et al.*, 2011, *MNRAS*, 413, 813
Cappellari,, M., McDermid,, R. M., Alatalo, K., *et al.* 2013, *MNRAS*, 432, 1862
Hopkins, P. F., Cox, T. J., Dutta, S. N., *et al.*, 2009, *ApJS*, 181, 135
Koleva, M., Prugniel, P., De Rijcke, S., & Zeilinger, W. W., 2011, *MNRAS*, 417, 1643
Krajnović, D., Emsellem, E., Cappellari, M., *et al.*, 2011, *MNRAS*, 414, 2923
Kuntschner, H., Emsellem, E., Bacon, R., *et al.*, 2006, *MNRAS*, 369, 497
Kuntschner, H., Emsellem, E., Bacon, R., *et al.*, 2010, *MNRAS*, 408, 97
McDermid, E., *et al.*, 2014, *MNRAS*, submitted
Rawle, T. D., Smith, R. J., & Lucey, J. R., 2010, *MNRAS*, 401, 852
Scott, N., Cappellari, M., Davies, R. L., *et al.*, 2013, *MNRAS*, 432, 1894
Spolaor, M., Kobayashi, C., Forbes, D. A., Couch, W. J., & Hau, G. K. T., 2010, *MNRAS*, 408, 272
Trager, S. C., Worthey, G., Faber, S. M., Burstein, D., & Gonzalez, J. J., 1998, *ApJS*, 116, 1

https://doi.org/10.1017/S1743921315003385 Published online by Cambridge University Press